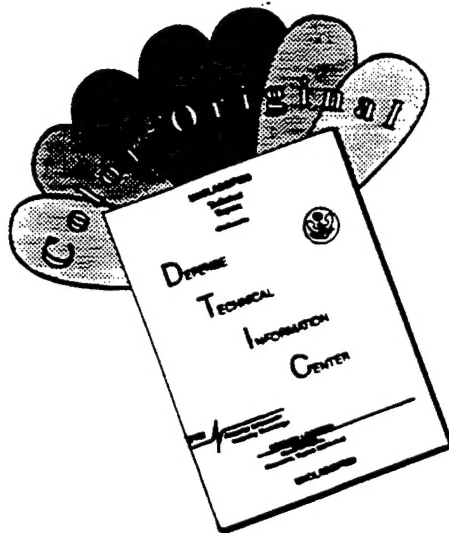

Quantitative Imaging of In-cylinder Processes by Multispectral Methods

C. Chang, E. Clasen, K. Song, S. Campbell and KT Rhee
Department of Mechanical and Aerospace Engineering
Rutgers, The State University of New Jersey
Piscataway, New Jersey

H. Jiang
Detroit Diesel Corporation
Detroit, Michigan

19970514 143

DISCLAIMER NOTICE



THIS DOCUMENT IS BEST QUALITY AVAILABLE. THE COPY FURNISHED TO DTIC CONTAINED A SIGNIFICANT NUMBER OF COLOR PAGES WHICH DO NOT REPRODUCE LEGIBLY ON BLACK AND WHITE MICROFICHE.

REPORT DOCUMENTATION PAGE			Form Approved OMB NO. 0704-0188	
Public reporting burden for this collection of information is estimated to average 1 hour per response, including the time for reviewing instructions, searching existing data sources, gathering and maintaining the data needed, and completing and reviewing the collection of information. Send comment regarding this burden estimate or any other aspect of this collection of information, including suggestions for reducing this burden, to Washington Headquarters Services, Directorate for Information Operations and Reports, 1215 Jefferson Davis Highway, Suite 1204, Arlington, VA 22202-4302, and to the Office of Management and Budget, Paperwork Reduction Project (0704-0188), Washington, DC 20503.				
1. AGENCY USE ONLY (Leave blank)		2. REPORT DATE		3. REPORT TYPE AND DATES COVERED Reprint
4. TITLE AND SUBTITLE Quantitative Imaging of In-cylinder Processes by Multispectral Methods			5. FUNDING NUMBERS DAAH04-95-1-0430	
6. AUTHOR(S) C. Chang, E. Clasen., K. Song, S. Campbell, H. Jiang and KT Rhee				
7. PERFORMING ORGANIZATION NAMES(S) AND ADDRESS(ES) Rutgers, The State University of New Jersey College of Engineering Mechanical and Aerospace Engineering Piscataway, NJ 08854			8. PERFORMING ORGANIZATION REPORT NUMBER	
9. SPONSORING / MONITORING AGENCY NAME(S) AND ADDRESS(ES) U.S. Army Research Office P.O. Box 12211 Research Triangle Park, NC 27709-2211			10. SPONSORING / MONITORING AGENCY REPORT NUMBER ARO 34452.2-EG	
11. SUPPLEMENTARY NOTES The views, opinions and/or findings contained in this report are those of the author(s) and should not be construed as an official Department of the Army position, policy or decision, unless so designated by other documentation.				
12a. DISTRIBUTION / AVAILABILITY STATEMENT Approved for public release; distribution unlimited.			12 b. DISTRIBUTION CODE	
13. ABSTRACT (Maximum 200 words) With the objective of achieving better investigation of engines-fuels by obtaining instantaneous quantitative imaging of in-cylinder processes, several steps have been taken for some years at Rutgers University. They are: (1) Construction of a new Multispectral high-speed infrared (IR) digital imaging system; (2) Development of spectrometric analysis methods; (3) Application of the above to real-world in-cylinder engine environments and simple flames. This paper reports some of results from these studies. The one-of-a-kind Rutgers IR imaging system was developed in order to simultaneously capture four geometrically (pixel-to-pixel) identical images in respective spectral bands of IR radiation issued from a combustion chamber at successive instants of time and high frame rates. In order to process the raw data gathered by this Rutgers system, three new spectrometric methods have been developed to date: (1) dual-band mapping method; (2) new band-ratio method; and (3) three-band iteration method. The former two methods were developed to obtain instantaneous distributions of temperature and water vapor concentrations, and the latter method is to simultaneously find those of temperature, water vapor and soot in gaseous mixtures, i.e., to achieve quantitative imaging. Applications of these techniques were made to both SI and CI engine combustion processes as well as bench-top burner flames. Discussion is made on the methods and new results.				
14. SUBJECT TERMS Quantitative Imaging, In-cylinder Processes, Super Imaging System, Instantaneous Distribution, Temperature and Species, Multispectral Methods			15. NUMBER OF PAGES	
17. SECURITY CLASSIFICATION OR REPORT UNCLASSIFIED			18. SECURITY CLASSIFICATION OF THIS PAGE UNCLASSIFIED	
19. SECURITY CLASSIFICATION OF ABSTRACT UNCLASSIFIED			20. LIMITATION OF ABSTRACT UL	

DTIC QUALITY INSPECTED 4

Quantitative Imaging of In-cylinder Processes by Multispectral Methods

C. Chang, E. Clasen, K. Song, S. Campbell and KT Rhee
Department of Mechanical and Aerospace Engineering
Rutgers, The State University of New Jersey
Piscataway, NJ 08855

H. Jiang
Detroit Diesel Corporation
Detroit, MI 48239

ABSTRACT

With the objective of achieving better investigation of engines-fuels by obtaining instantaneous quantitative imaging of in-cylinder processes, several steps have been taken for some years at Rutgers University. They are: (1) Construction of a new multispectral high-speed infrared (IR) digital imaging system; (2) Development of spectrometric analysis methods; (3) Application of the above to real-world in-cylinder engine environments and simple flames. This paper reports some of results from these studies.

The one-of-a-kind Rutgers IR imaging system was developed in order to simultaneously capture four geometrically (pixel-to-pixel) identical images in respective spectral bands of IR radiation issued from a combustion chamber at successive instants of time and high frame rates.

In order to process the raw data gathered by this Rutgers system, three new spectrometric methods have been developed to date: (1) dual-band mapping method; (2) new band-ratio method; and (3) three-band iteration method. The former two methods were developed to obtain instantaneous distributions of temperature and water vapor concentrations, and the latter method is to simultaneously find those of temperature, water vapor and soot in gaseous mixtures, i.e., to achieve quantitative imaging.

Applications of these techniques were made to both SI and CI engine combustion processes as well as bench-top burner flames. Discussion is made on the methods and new results.

INTRODUCTION

BACKGROUND. Investigating how design-operation and fuel variables affect in-cylinder events, a question may arise: What in-cylinder information would be most desirable when experimentally studying the reaction processes?

A plausible answer to this question, which is perhaps as old as the advent of the internal combustion engines (ICE), is considered here. That is, in order to improve our understanding of the reactions, it would be desirable to obtain instantaneous distributions of temperature and species within the combustion chamber at successive instants of time. Such pieces of information may be referred to as "quantitative images." When they are made available, there is no doubt that a better understanding about the engine can be achieved, including the thermal budget, knock and even emissions. This goal, in fact, has been sought after by many auto-engineers using various methods such as different probes and electro-optical diagnostic methods in the past. While their measurement were made mostly at a limited number of points at a time, (visible-ray) photos obtained of combustion processes at high rates have helped in gaining a global understanding of the in-cylinder phenomena.

Realizing powerful advances in modern sensors and data processing technologies, a new approach of ICE-research was initiated at Rutgers University some years ago in order to achieve the goal of quantitative imaging as extensive as possible. This approach is, in a sense, an attempt of gaining multiple effects expected when both methodologies of point measurements and cinematography are combined together. This paper reports the new research methods and some of recent results obtained from the work.

PREVIOUS STUDIES. Several earlier studies relevant to the present work are discussed at first. They are summarized in Fig. 1 along with new methods to be discussed here. It was 1947 when Uyehara and Myers [1]* first reported a laboratory-built two-color (emission spectrometry) measurement system applied to determination of the instantaneous flame temperature in a Diesel engine

*Numbers in parentheses designate references at end of paper.

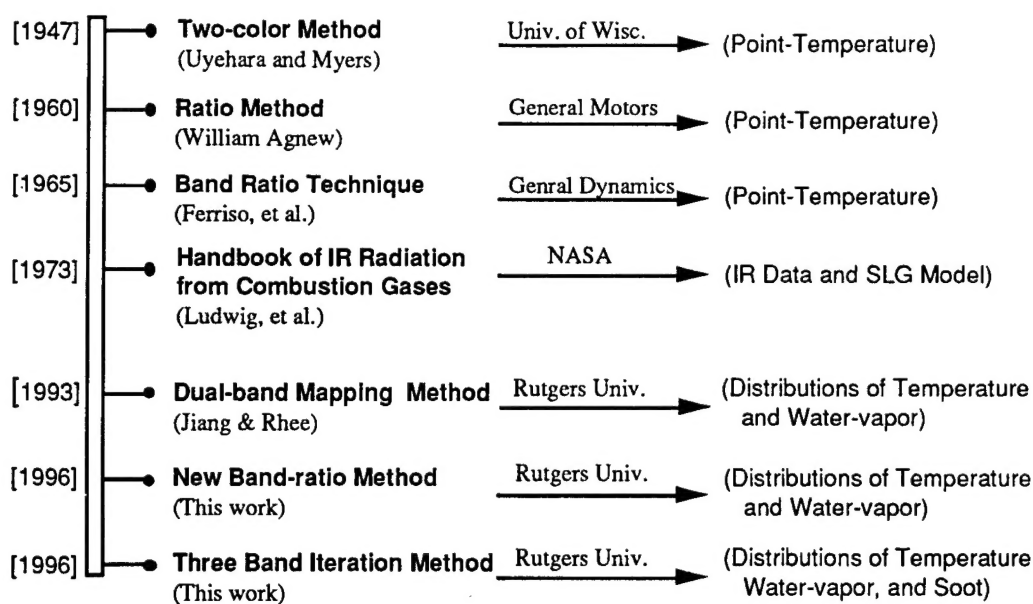


Figure 1. Multiple-band Spectrometric Methods for Temperature and Species Measurement in Flames.

combustion chamber. The basic concept of this new technique was the ratio of spectral radiation intensities of soot was directly related to the flame temperature, which assumed that soot was a gray-body and that radiation from gaseous species was negligible via two bands they employed. Note that a similar methodology was employed by others in later years [2]. They continued to develop new two-color (absorption spectrometry) methods for in-cylinder temperature measurement by employing sodium vapor [3] and water vapor [4] as radiatively participating species.

The concept of the ratio method was also introduced in 1960 by William Agnew [5] to determine temperatures of the end gas in an SI engine (near the peak). In this emission spectrometry method, he indicated that two readings from detectors receiving respective spectral radiations by water vapor in a laboratory flame was related to the mixture temperature. The ratio method was explained by using the Plank's equation,

$$E = C_1 / \lambda^5 [\exp (C_2/\lambda T)-1] \quad (1)$$

where, C_1 and C_2 are constants. The concept of the method, again, was that the ratio of the emissive powers at two wavelengths, E_1/E_2 was a function of temperature only, which in his method was experimentally determined for a working relationship,

$$E_1/E_2 = [D_1/D_2] (K_2/K_1) [\epsilon_2/\epsilon_1] \quad (2)$$

where, D is the output of the detector and K is the relative sensitivity of the detector system via each wave band of λ .

In the above equations, K_2/K_1 and ϵ_2/ϵ_1 were determined by calibration using a bench-top burner apparatus, and D_1/D_2 was the experimental measurement relating to

temperature of the mixture. Two wavelengths employed in his method were those for receiving radiation from water vapor, $1.89\mu\text{m}$ and $2.55\mu\text{m}$. Note that his calibration was done to relate the ratio of detector readings to temperature closer to the peak value along the line of sight in the flame.

In 1965, Ferriso, et al. [6] introduced a so-called band-ratio technique (BRT), which was similar to the ratio method by Uyehara and Myers, and Agnew. They, however, employed measurements of radiation via rather wide band filters, namely: (A) $2.63\text{-}3.3\mu\text{m}$; (B) $2.3\text{-}2.63\mu\text{m}$; (C) $1.7\text{-}2.3\mu\text{m}$; and (D) $1.3\text{-}1.7\mu\text{m}$. They experimentally demonstrated that ratios of detector signal output (i.e., $\theta_{C/B}$, $\theta_{D/C}$, and $\theta_{D/B}$) were related to the exhaust gas temperature from a rocket motor. What is to be mentioned here is that since the band widths were so wide, their measurements involved radiation from more than one species in the combustion products. This may be one of the reasons why the relationships of θ vs. T were relatively crude [6], which is further discussed later.

Thanks to NASA Handbook (SP-3080) of infrared (IR) radiation (of gaseous mixtures) provided by Ludwig, et al. [7] in 1973, which contains the spectral absorption coefficients of individual gaseous species at varied temperatures and pressures, more meaningful work became possible. Agnew in 1960 probably did not have access to such data when he conceived his ratio method so that he resorted to experimental means in order to obtain the working calibration curve for his system.

After developing a new high-speed two-color IR imaging system at Rutgers [8, 9], which was to simultaneously capture two geometrically identical images in respective spectral bands, results from the NASA IR data and single-line-group (SLG) model [7] were employed in order to develop a new dual-band mapping method (DBMM). In an earlier paper [10], without giving a detailed

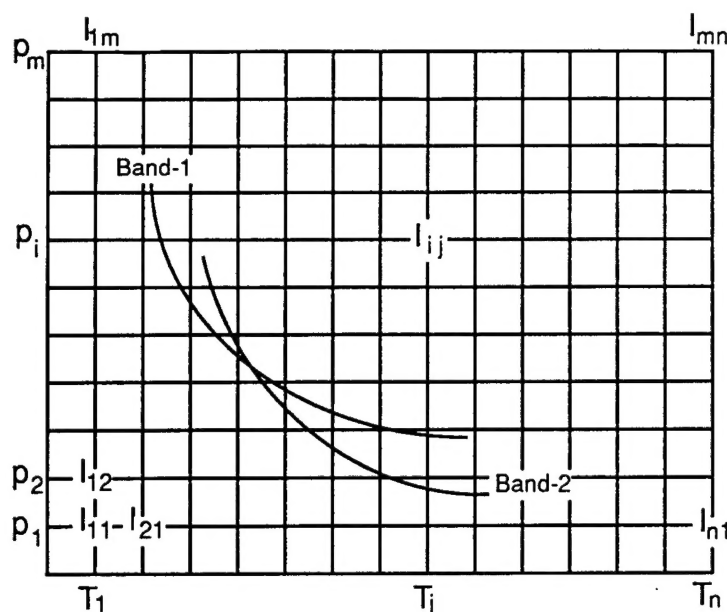


Figure 2. Algorithm for Dual-band Mapping Method (DBMM).

elaboration of the method, distributions of temperature and water vapor concentration obtained by this method were reported. In the following, the DBMM is discussed in comparison with other methods developed during the course of the present work.

RUTGERS SPECTROMETRIC METHODS AND RESULTS

DUAL-BAND MAPPING METHOD (DBMM). When a volume of uniform gaseous mixture in a known concentration of source (target) species having a given physical thickness is at a specified temperature and pressure, it is possible to calculate the spectral radiation intensities of the mixture. The core of the DBMM is to find temperature and species concentration in such a mixture when two spectral intensities are given, a reverse process of the former.

In order to achieve this goal, a new algorithm was developed as discussed by using a spectral intensity matrix (I_{ij}) of the mixture (Fig. 2), which covers, for a given wave band (Band-1), in a range of varied partial pressure of water vapor (p_i) and temperature (T_j). Then, an iso-intensity line is traced over this matrix according to the spectral intensity measured from the experiment. Then the same is made for the intensity matrix for another band (Band-2), and overlap these two matrixes with each other in order to find the crossing point of both iso-intensity lines. This is like finding two unknowns from two simultaneous equations.

In spite of the straight-forward concept of this method, error in the final result is likely to be high due to the two somewhat mutually paralleling lines as seen from Fig. 2. Even a small uncertainty in measurement would lead to a rather large error in the results. Furthermore, since the physical length of individual optical paths through a real-world flame is difficult to determine, the error could increase more. It is noted again, in spite of such limitations stemming

from probable imperfect measurements, the results obtained by this method are unique. A sample result is shown when a new band-ratio method is explained later.

RUTGERS FOUR-COLOR IMAGING SYSTEM.

Prior to discussing other spectrometric methods, the Rutgers high-speed four-band IR digital imaging system (referred to as the Rutgers System or Super Imaging System, SIS) is explained. While the abovementioned two-color system continued to be used for flame and engine studies [8-11], and also for implementation of the DBMM [10], an entirely new system was developed as schematically shown in Fig. 3. Since this SIS was described earlier [12-14], it is only briefly explained here.

Referring to Fig. 3, the radiation from an object is collected by the cassegrain assembly (152mm diameter), which is spectrally split to place four spectral images over respective high-speed digital imaging units. The SIS, therefore, can be used to simultaneously obtain four separate sets of 64x64 digital image in corresponding spectral bands. Ideally, images of four different pieces of information can be obtained at successive crank angles (CA).

While the spectrometric techniques were being developed for achieving quantitative imaging by processing the digital data captured using the SIS, the main topic of the present paper, the raw results alone have been useful in finding some new observations. They include: preflame reactions [11-14]; liquid-fuel layers over the cylinder head surface; and postflame oxidation [12,13], which were not reported earlier by others.

NEW BAND RATIO METHOD. The computer program developed for the abovementioned DBMM, which contained spectral absorption coefficient data under varied temperatures and total pressures, and incorporated with the SLG model, was further improved. The SLG model from

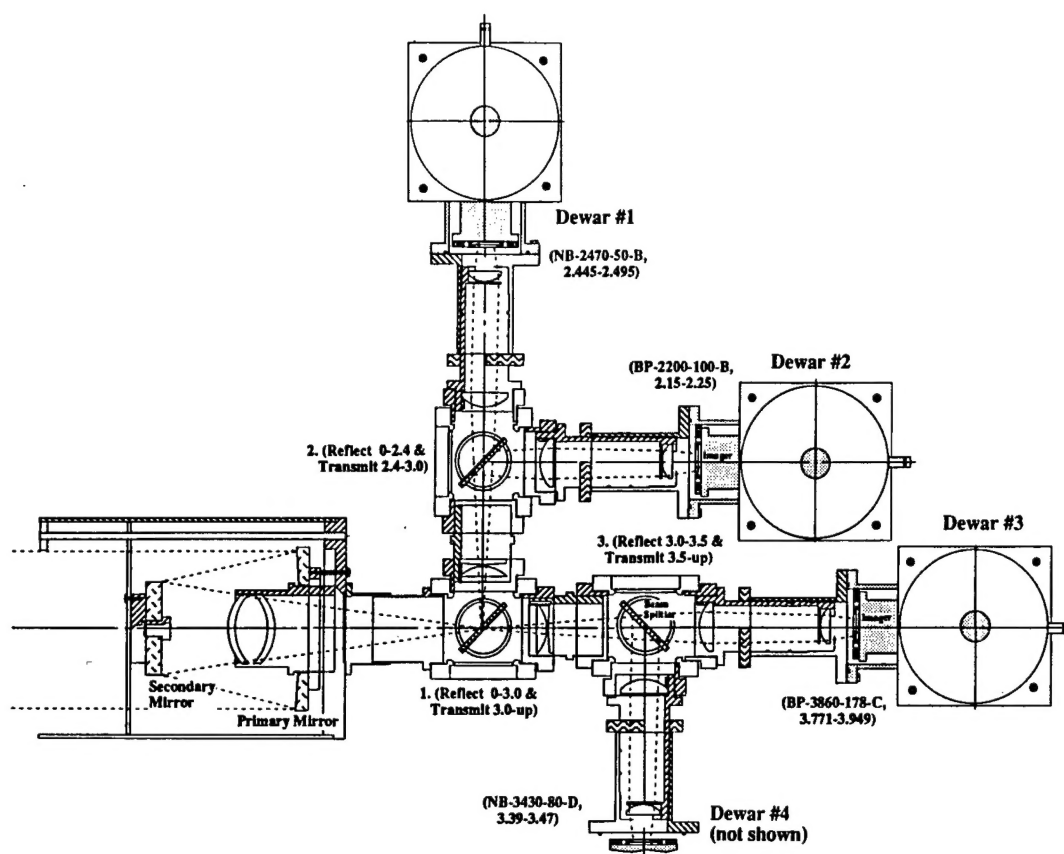


Figure 3. Schematic Presentation of Optical Portion of Rutgers SIS.

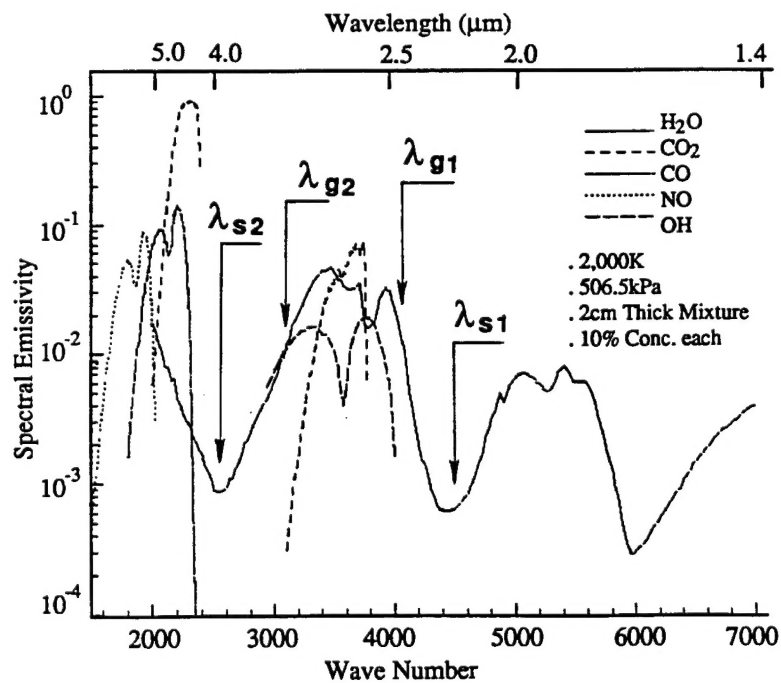


Figure 4. Spectrogram Constructed by using Rutgers DBCP for a Gaseous Mixture.

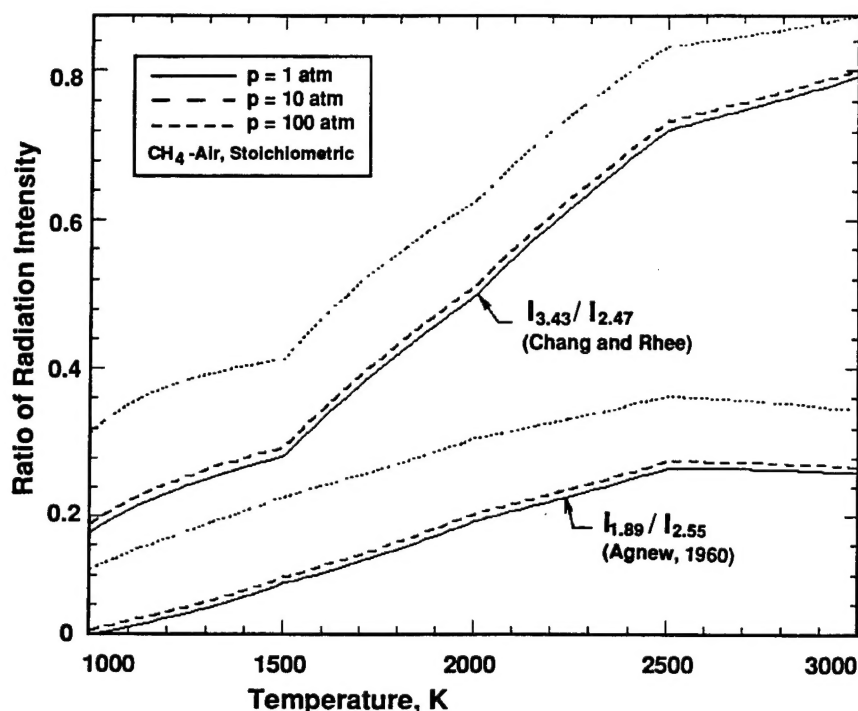


Figure 5. New Band Ratio Method (NBRM) to Determine Temperature in Gaseous Mixtures.

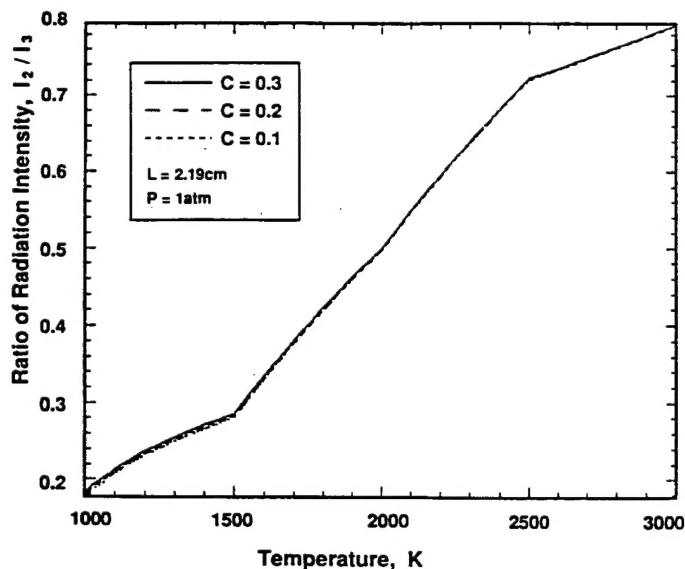
NASA's IR handbook [7] was to facilitate utilization of those absorption coefficients given for each wavenumber, such as for calculation of the spectral radiation intensity and emissivity of a specified gaseous mixture. For example, Fig. 4 was prepared by using this data-based computer program (DBCP). This was done for a sample gaseous mixture (thickness 2cm) composed of H_2O , CO_2 , CO , NO , and OH with concentration $C=0.1$ in mole fraction each under pressure, $P=10\text{atm}$. The figure suggests that bands at $2.47\mu\text{m}$ and $3.43\mu\text{m}$ have strong radiation by water vapor, which are employed in the following spectrometric method. Development of this DBCP paved the way to the analysis of spectral characteristics of radiating species in the present IR domain to come up with the new band-ratio method (NBRM), as shown in Fig. 5.

The figure is self-explanatory and it indeed supports Agnew's earlier experimental work and Ferriso's BRT measurement method. It is noted that this result was constructed by the abovementioned DBCP to relate the ratio of spectral intensities from mixture containing a target species to temperature of the mixture under a specified total pressure. No experimental factor is involved in the result.

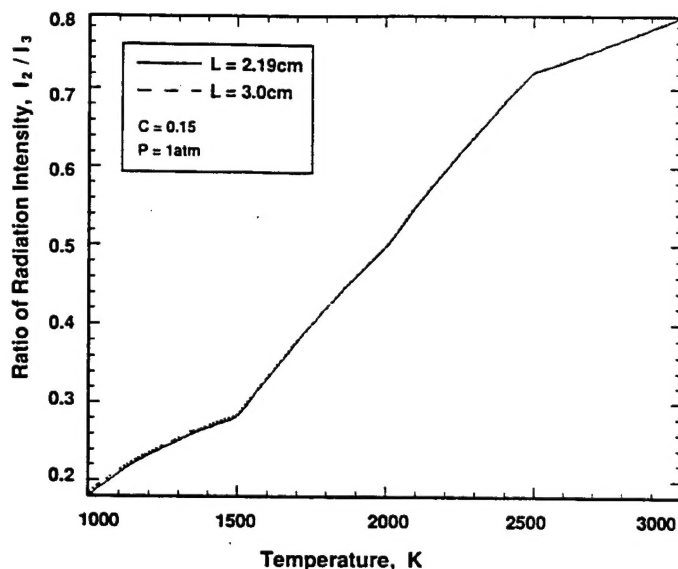
There are several new features in the NBRM: (1) It includes the pressure effects on the relationship, which neither Agnew nor Ferriso, et al. considered in their methods; (2) The method employs a single radiatively participating species; (3) Its band widths are narrow to improve the accuracy; (4) The analysis permits identification of a pair of desirable bands for achieving more accurate temperature determination; and (5) The relationship is universally applicable unlike the detection system-dependent curves generated via experiment [5,6].

Regarding the pressure effect on the NBRM, Fig. 5 indicates how significant it may be when reactions under varying pressure are considered such as in an engine cylinder. The NBRM was applied to two wave bands employed by Agnew [5] as shown by the solid-line, which is compared with dotted curves for high pressures in the same figure. This illustrates the NBRM's need for incorporating the effect of reaction pressure in order to obtain accurate temperature results. In selecting bands (i.e., filters in experiment) for the NBRM, it is desirable for them to pass radiation from only a single source species. For example, when this method is applied to a hydrogen-air flame, not only the selection of bands will be simple but also the measurement accuracy will be high because there is only water vapor emitting IR radiation in the product. When bands which permit some strong radiation by additional species (e.g. carbon dioxide and/or soot) to pass together with radiation from the target species (here, water vapor) were employed by the NBRM, the relationship in Fig. 5 was not unique indicating errors to be made in measurements. Recall that, since wide bands tend to include radiations from more species, those employed for the Ferriso's BRT were considered to be inappropriate.

In typical hydrocarbon-air flames, many species including intermediate species are formed and also consumed, which radiate more or less in the IR band domain. They can not be considered all in a simple spectrodiagram shown in Fig. 4. Even a narrow band rarely passes radiation by only a single species without interference by others. If such interference is not negligible, the accuracy will suffer. Note that the accuracy will be enhanced, however, when additional bands (for corresponding species, otherwise



(A)



(B)

Figure 6. Characteristics of New Band Ratio Method Indicating Minimum Dependency of: (A) Species Concentration and (B) Path Length.

causing interference) are employed, which is demonstrated by the new method as discussed later.

When two solid lines in Fig. 5 are compared with each other, the measurement accuracy is expected to be higher for a steeper curve, which suggests the selection of a proper pair of bands to be important in the NBRM. The last statement is reiterated because unlike the voltage measurements out of the sensors employed by others in the past, the present method is to find temperature from intensities of the mixture, which is independent of the system response, e.g. values of K in Eq. (2).

Additional analyses revealed that the relationship (Fig. 5) was found to be quite independent of the species concentration and physical length of the optical depth, as shown in Fig. 6. These characteristics are very important in applying the NBRM in the typical combustion environment where concentration and flame thickness vary greatly along the line of sight. These results illustrate that ϵ_2/ϵ_1 in EQ (2) is not affected by the variation of concentration and optical length, L . It becomes reasonable if the optical thickness is relatively small as seen from the Beer's law, $\epsilon = 1 - \exp(-\kappa L)$. That is, when κL is very small, $\epsilon \sim \kappa L$. Note that κL is indeed small in many combustion environments, which is optically thin, except for soot-laden flames whose solution is considered by another method later.

CALIBRATION. At this time, the method of the system calibration for determining spectral intensities from the digital images is explained. The purpose of this calibration is to accurately measure, for individual pixels, the radiation intensity of a (target) mixture (either in a bench-top flame or engine cylinder). Note that the ratio relationship

to temperature (Fig. 5) needs no calibration. For this, the imaging system is placed at exactly the same geometric orientation with respect to the target as in the actual (engine) experiment. Then, the digital output from pixels are compared with those obtained when the target is replaced by a blackbody at a known temperature. The conversion matrixes of the system-response permit the construction of spectral intensity distribution at the target using the raw data, i.e.,

$$I_{ij} = a_{ij} v_{ij} + b_{ij}, \quad (3)$$

where, v is digital output in voltage. Note that the system response in Eq. (3) includes the combined effects of: (1) optical window in the engine; (2) optical elements in Fig. 3; (3) individual pixels; (4) the location of pixel with respect to the axis of the path; and (5) electronic components. Since the need for such characterization is well known, no further elaboration is made here.

In addition, effects of deposit formation over the optical window on the measurement is discussed. While in visible range imaging, even a small amount of window deposit degrades the image quality, which occurs within a short period of engine operation, imaging in the present IR domain is found to be lightly affected by the deposit. For example, the quality of in-cylinder image obtained of a gasoline-operated SI engine, after more than 20 minutes of continuous operation (without cleaning the IR window) from the (cold) start, still appeared to be reasonably good [13]. Similar insensitivity was also found in imaging of a reacting spray plume of a direct injection CI engine [11,14]. Such a high transmission of IR radiation through the deposit-layered window, however, does not necessarily guarantee accurate quantitative imaging. On the other hand, the ratio method of

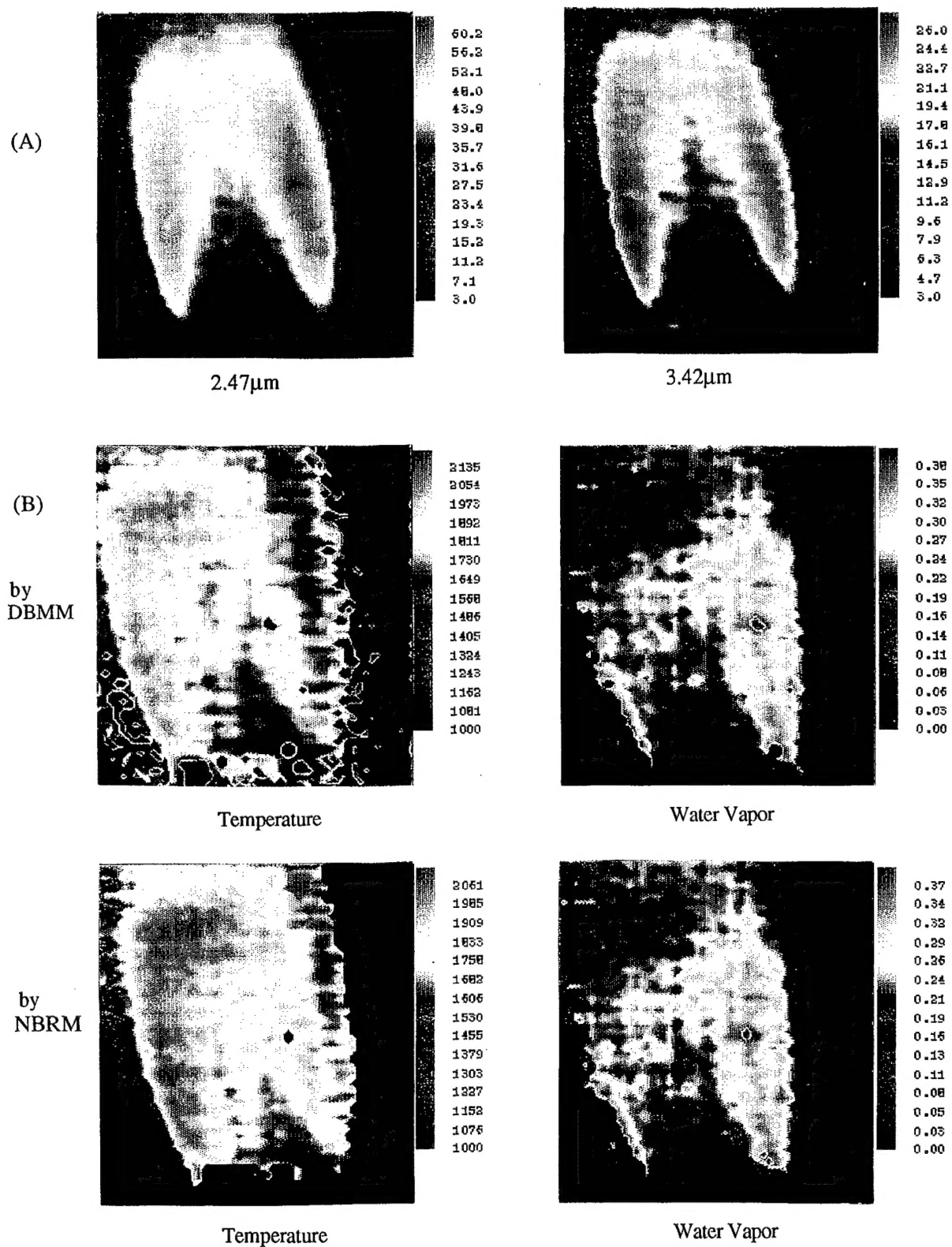


Fig. 7. (A) Spectrometric Intensity Images of a Hydrogen-air Flame in 2.47 μ m and 3.42 μ m, and (B) Distributions of Temperature (K) and Water Vapor (atm-cm) by DBMM and NBRM.

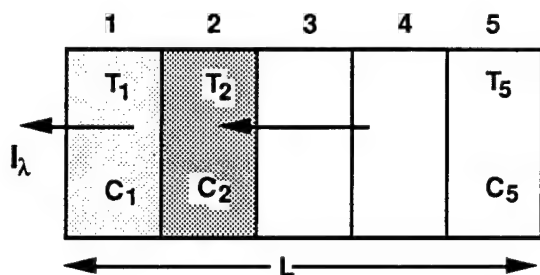


Figure 8. A Case Analyses of a Flame with Designated Temperature and Water Vapor Concentration.

processing spectral IR data has advantages over others such as single-band imaging, because effects due to either absorption or emission (by the deposit) on both band measurements would tend to cancel each other minimizing the error.

SAMPLE RESULTS BY NEW SPECTROMETRIC METHODS. A set of results obtained by using the DBMM and NBRM is shown in Fig. 7. The spectral IR radiation images of a hydrogen-air diffusion flame in bands of 2.47 μm and 3.43 μm were obtained (Fig. 7-(A)) from a setup, which is a duplicate of a laminar-flow burner employed by Lewis and von Elbe [10,15]. The raw data was processed to construct intensity images by using system response matrix (Eq. 3) in order to achieve quantitative imaging by the methods. Shown in Fig. 7-(B) are the temperature distribution (TD) in K, and water vapor distribution (WVD) in atm-cm determined by using the DBMM and the NBRM, respectively. Once the TD is determined, since the emissivity is calculated using the Plank's equation, the WVD is found using the Rutgers DBCP mentioned earlier. The presentation is made in pseudo-color in order to display more local variations.

It is pointed out that the distributions are two-dimensional as seen by the imaging system, and that each point measurement, within the matrix, represents that of the corresponding line of sight in the direction perpendicular to the image plane. The two methods produce mutually comparable results except for the border zones where the DBMM overestimates the temperature. This is found to occur due to an assumption of the identical flame thickness throughout the flame in DBMM, which is not realistic because it is small around the border.

In spite of differences between flames by the present DBMM / NBRM experiment and Lewis and von Elbe [15], (For example, one was an instantaneous measurement and the other was a time-averaged local measurement using the sodium-line reversal method, and also fuel) the results are mutually comparable each other. The absence of a similar result in literature, however, did not facilitate any further evaluation of the WVD.

WHAT TEMPERATURE? When the target mixture is uniformly mixed, the temperature determined by using the present ratio method would be the same at any point over the mixture. The temperature along the line of sight, however,

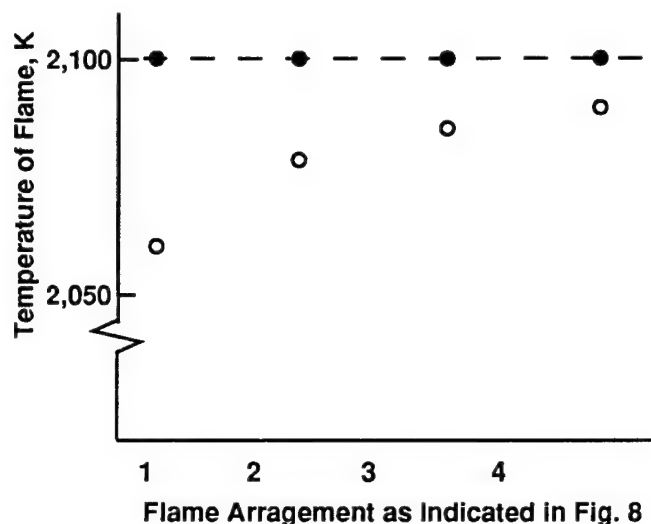


Figure 9. Temperature Determination by NBRM for various Flame Configurations.

varies in most combustion products so that the nature of measurements obtained by the method needs a discussion. A question comes to mind as to whether it is either close to the average temperature, or the highest temperature of the mixture somewhere along the line of sight, or other values. The same issue was also addressed in earlier studies [3,4].

In order to resolve the above question, the temperature determined by the NBRM was evaluated by using a simplified flame configurations as described in Fig. 8. The flame is assumed to consist five equal-thickness segments within the total thickness L having respective uniform temperatures (T_i) and water-vapor concentrations (C_i). Spectral radiation intensity at one side of the flame, I_λ will be a result of emission-transmission of individual segments as determined by

$$I_\lambda = I_{\lambda_1} + \tau_{\lambda_1} I_{\lambda_2} + \tau_{\lambda_1} \tau_{\lambda_2} I_{\lambda_3} + \dots$$

$$= \sum_{i=1}^n \left(\prod_{m=1}^{i-1} \tau_{\lambda_m} I_{\lambda_i} \right) \quad (4)$$

Note that, in the radiative participation by these mixtures, the absorption of radiation by a segment, as issued from others, is included to affect its thermal budget, as specified at each segment. In this analysis, for the sake of simplicity the temperature considered in each segment is assumed to be the result of various processes including such absorption.

In this evaluation, two spectral intensities (via wave bands of 2.47 μm and 3.43 μm) are determined by using Eq. (4) and the Rutgers DBCP. The ratio of these two, then, are used for finding temperature by the NBRM for several cases as considered next. Note that the flame thickness $L = 2\text{cm}$ and the total pressure $p = 1\text{atm}$.

Results are shown in Fig. 9 for the following flame configurations: "1" in flame arrangement indicates a mixture of combustion product when segment-2 is occupied by a mixture at 2,100K with water vapor concentration $C = 0.12$ and other segments are with radiatively transparent species;

"2" means when segments-2 and-3 are filled with the same mixture; and so forth. For these cases, the NBRM determines exactly the same temperature, as indicated by the filled-in dots, which proves that the method is valid at least for such a uniform mixture.

On the other hand, since the flame is not uniform in general, other cases were considered, including those as same as the above but having segment-1 filled with a mixture at 1,100K and $C=0.06$. Results for these cases are indicated by open-dots in the figure. Important characteristics of temperature by the NBRM deduced from this analysis may be listed: (1) The temperature determined by the method is quite close to the peak temperature; (2) When the water vapor concentration is high in the segment with the peak temperature, the determination is closer to the peak value; and (3) The effect of low-temperature mixtures in a flame (e.g. segment-1) on the measured temperature may be significant in some cases.

THREE-BAND ITERATION METHOD (TBIM).

The NBRM can be applied to relatively "clean" flames with minimum soot formation. There are many flames, however, containing significant amounts of soot emitting strong radiation, which defeats the application of the NBRM. A new three-band iteration method (TBIM) was developed for such cases. This method permits simultaneous determination of distributions of temperature, water-vapor and soot in combustion products as explained next.

Figure 10 is introduced in order to discuss the basic concept of the TBIM, which is similar to Fig. 5 and assumes to have only water vapor and carbon dioxide in the mixture. The lowest curve in the figure indicates the spectral intensity of combustion products from a hydrocarbon ($H/C=2$)-air mixture to produce a water vapor concentration, $C=0.10$ (for 2,000K and 1 atm), which was constructed by using the DBCP. Other upper curves represent the radiation from the same mixture containing soot as specified by given volume fractions, f_v . In this method, in addition to two unknowns as considered earlier by the NBRM, one more affecting the emissivity of a mixture is determined, which is to find the absorption coefficient of the soot using the Rayleigh-limit expression [16,17],

$$\kappa_{s\lambda} = \frac{36n^2k(\pi/\lambda)f_v}{[n^2(1-k^2)+2]^2+4n^4k^2} \quad (5)$$

where, n , nk are complex refraction indices of soot determined by the dispersion equation [18].

The governing equations for the problems, therefore, are established Beer's Law for three spectral bands, namely 3.8 μ m, 2.47 μ m, and 3.42 μ m as:

$$\begin{aligned} \epsilon_{380T} &= 1 - \exp(-\chi_{380S} - \chi_{380H}) \\ \epsilon_{247T} &= 1 - \exp(-\chi_{247S} - \chi_{247H}) \\ \epsilon_{342T} &= 1 - \exp(-\chi_{342S} - \chi_{342H}) \end{aligned} \quad (6)$$

where,

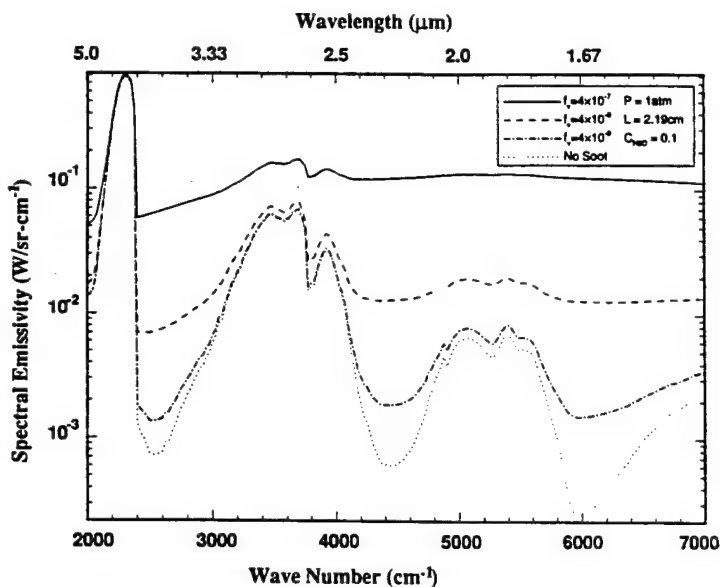


Figure 10. Spectrodiagram of Combustion Products of a Hydrocarbon-air Flame with Soot.

$$\chi_{380S} = \kappa_{\lambda} L / 3.80^{\alpha}$$

$$\chi_{247S} = \kappa_{\lambda} L / 2.47^{\alpha}$$

$$\chi_{342S} = \kappa_{\lambda} L / 3.42^{\alpha}$$

and $\alpha=0.95-1.0$ [19]. Note that the final results are found to be insensitive to the value of semiempirical constant, α . Here, χ for water vapor (at different temperatures and pressures) is determined from the DBCP. In the equation, the roles by soot and water vapor are denoted by subcharacters, S and H, respectively.

Mentioning the iteration method for finding the solution, Fig. 11 is offered here. Although the radiation from water vapor is small in 3.8 μ m band in low pressure reactions, the effect is, nevertheless, included in the present TBIM in order to minimize the error particularly in high pressures. In the calculation, at first, measurements via 3.42 μ m and 2.47 μ m are assumed to be free of soot radiation to use the NBRM for determining the initial value of flame temperature. Next, the extinction coefficient, χ by water vapor is calculated, which is reflected on determination of κL on 3.8 μ m band. The κL effect is then subtracted from χ for the two bands used for the initial estimation of temperature. The new temperature calculation by the NBRM for the two band, then, becomes more accurate than the initial estimate. The next steps are for improving the accuracy by going back to calculation of the extinction coefficient of water vapor for 3.8 μ m band. The iteration process is continued until a converging temperature value is found.

RESULTS OBTAINED BY TBIM. This new method was applied to the measurement of a bench-top burner and in-cylinder mixtures of a (cold) gasoline SI engine and a Diesel oil (D-2) operated direct injection (DI) CI engine.

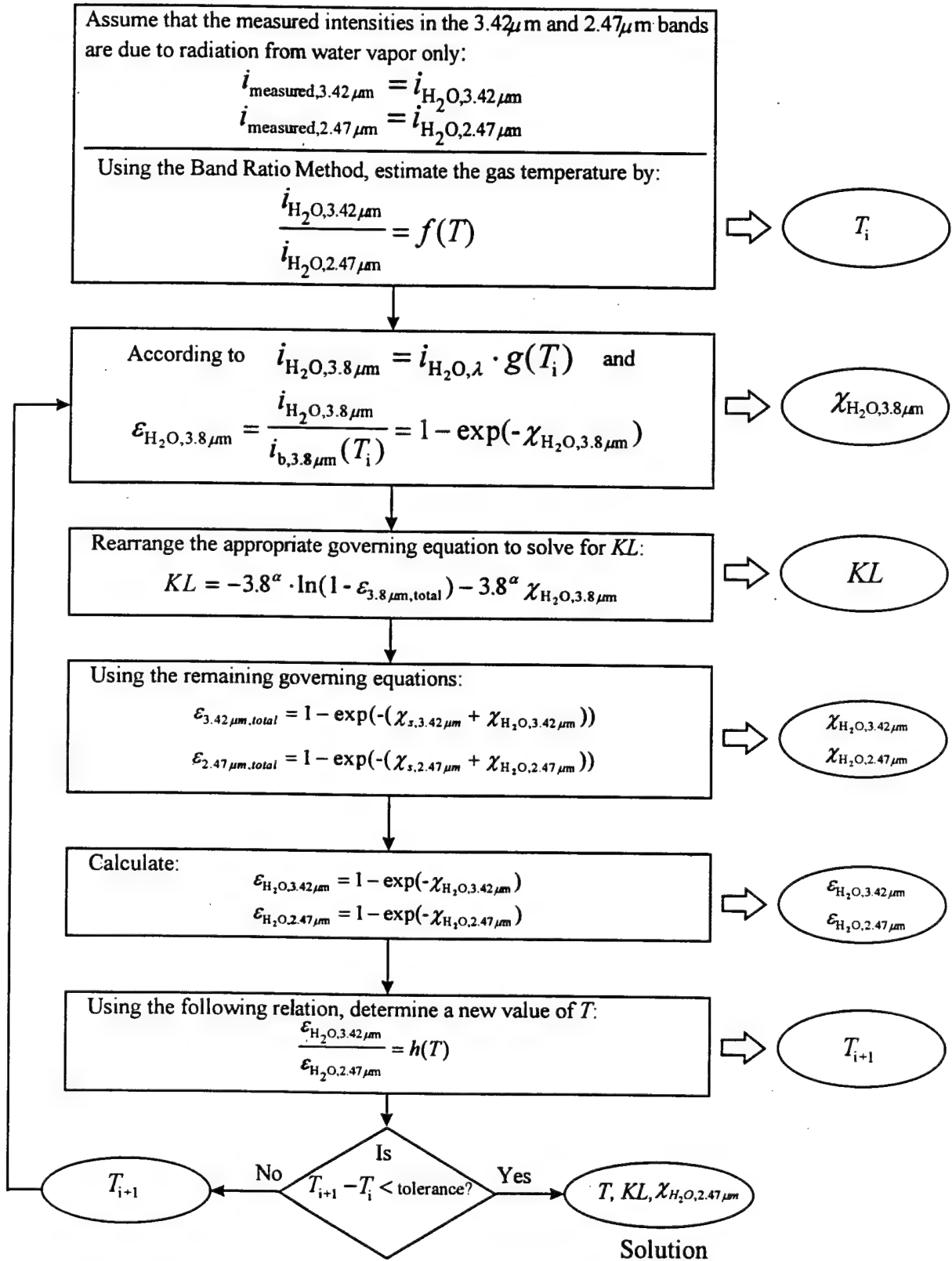


Figure 11. Flow-chart for the TBIM applied to Soot-laden Hydrocarbon-air flame.

Prior to presenting some results from the CI study, a short description of the experimental apparatus is made here. More details may be found elsewhere [11,14]. A single-cylinder DI-CI engine was mated with a section of Cummins 903 four-valve cylinder head where a high-pressure electronically-controlled injection system was installed. For imaging, one of the intake valves was replaced by an optical access (37mm diameter), which is barely big enough to observe one of eight sprays made through nozzle holes with 0.15mm diameter. The high-pressure injection system used in this experiment is basically a BKM's Servo-jet type [20]. In order to achieve versatility of the system, however, almost the entire unit was newly fabricated at Rutgers [11,14] to operate at pressures over 165MPa. The imaging, therefore, was made through the cylinder head to look down the spray from the top. In addition to gathering of raw spectral digital images by the SIS, other engine data were also collected, including the matching pressure-time data as required by the NBRM, which is a part of the TBIM.

The raw data matrixes were converted to corresponding spectral intensity distributions by using the calibration method as explained earlier. Figure 12-(A) shows these intensity images of a spray plume at successive CA with injection starting at 9CA before the top-dead-center (bTDC) as indicated by a look-up-table (LUT) shown in Fig. 13. The spray is directed diagonally as indicated by the arrow mark shown in box for 5.5CA bTDC. They are in bands of $2.47\mu\text{m}$, $3.42\mu\text{m}$ and $3.80\mu\text{m}$, which were to capture radiation from water vapor and soot assuming interference from other species is negligible (refer to spectrodiagrams shown in Figs. 4 and 5).

Discussing the spectral intensity images, the first image of spray was captured *immediately* after the fuel injection via $3.42\mu\text{m}$ band, which was reported earlier [11,14]. This new observation was explained by chemiluminescent radiation issued by some unknown species, which may include OH, CH, C_2 , aldehydes, and others expected in preflame reactions during the ignition delay period. The new finding seems to be reasonable because the fuel-air mixture undergoes many elementary reactions prior to exhibiting explosive (visible) premixed flame reactions, and because the early mixture formation occurs at injection. The first images obtained via other bands, i.e., at $2.2\mu\text{m}$, $2.47\mu\text{m}$ and $3.80\mu\text{m}$ were all found at the same CA, which was captured in this case at 5.5CA bTDC. (This is far after finding the first preflame image in $3.42\mu\text{m}$ band around 9CA bTDC.) They represent the onset of the premixed combustion stage. In a great amount of results, where the first preflame zones were observed in the spray, there also the first premixed reaction center appeared. In some cases, however, the two zones do not necessarily match each other, which warrants further investigation.

In general, the spectral intensity distributions are somewhat different from each other particularly in the early stage of combustion, which is until around 1.5 after TDC. Thereafter the images in $2.47\mu\text{m}$ and $3.42\mu\text{m}$ are similar each other, which differs from that in $3.8\mu\text{m}$. The similarity of images representing radiation by water vapor in the later stage of combustion is explained by the negligible amount of radiation by other species expected then, which is opposite in


 -5.5	-2.0	1.5	5.0	8.5
12.0	15.5	19.0	22.5	26.0

Fig. 13. Look-up-Table for Fig 12.

the early stage of combustion indicating many different species presenting to issue individual radiations.

The TBIM was employed to obtain distributions of temperature (K), water vapor (atm-cm) and soot (κL) by processing the abovementioned spectral intensity data, as shown in Fig. 12-(B). In order to construct the quantitative images, digital results were plotted according to corresponding color strips, for which several observations may be listed: (1) The numbers quantifying the characteristics of Diesel spray-plume combustion by high-pressure injection seem to be reasonable; (2) The local variation is continuous without abrupt changes except for those in the early stage of combustion; (3) The progress of reactions with time are smooth and gradual; and (4) No solution was obtainable for those in the early stage of combustion.

In addition to the absence of complexity in calibration, well-established governing equations and spectral absorption data from the handbook, as employed in the TBIM, the above observations seem to help trust the validity of the results. The quantitative images (e.g. distributions of temperature, κL and water vapor) are within values reported by others, except for low κL in the present measurement compared with those by mechanical injectors, which may be explained by the low-soot formation characteristics by the high-pressure injection system. The absence of abrupt local variation over the same quantitative image is expected in the continuum flow in the later stage of combustion. Similarly, the smooth changes in the distributions with time are expected in a progressively reacting spray. The inability of finding solutions in the early stage of combustion by the TBIM is also reasonable and compatible with the other observations. This is because the many intermediate species produced in the stage (recall the preflame images via $3.42\mu\text{m}$ band, for example) are expected to emit radiations added to those by water vapor and soot. Misrepresentation of spectral intensity measurements due to such interferences drove the iteration process of solution out of convergence, as indicated by the black zones in the results. (It is reminded that measurements of combined radiation from multiple species will cause erroneous results unless they are all included via additional governing equations, and corresponding spectral image data). These observations are not sufficient conditions for confirming the full validity of results, but certainly required conditions.

Reviewing the direction of spray (Fig. 13), the results in Fig. 12 indicate the region along the axis of spray is at low temperature, which was similarly found in combustion of spray by a mechanical injector [21]. The low-temperature

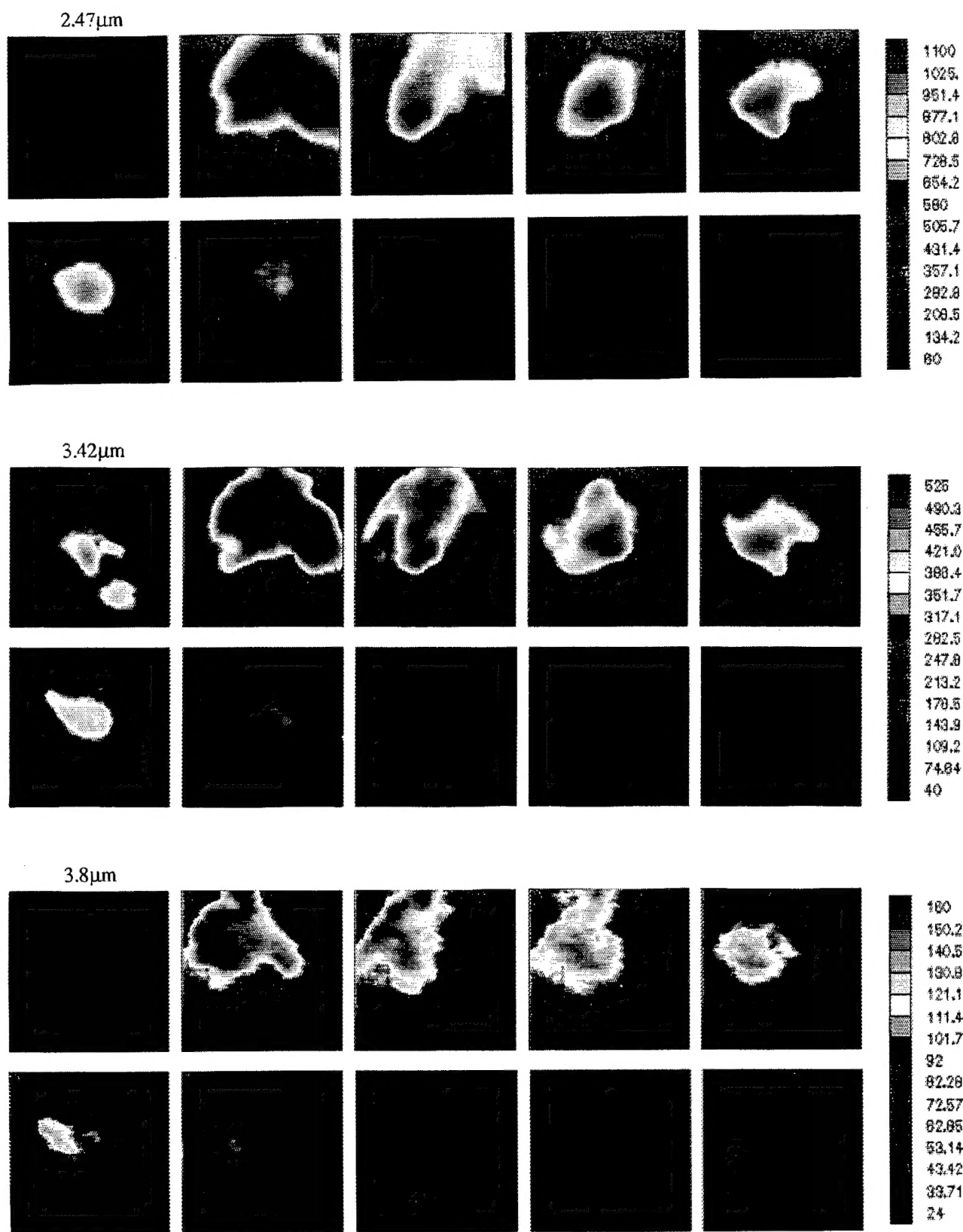


Figure 12. (A) Spectrometric Intensity Image of a Spray-plume in a DI-CI Engine at Successive Crank Angles.

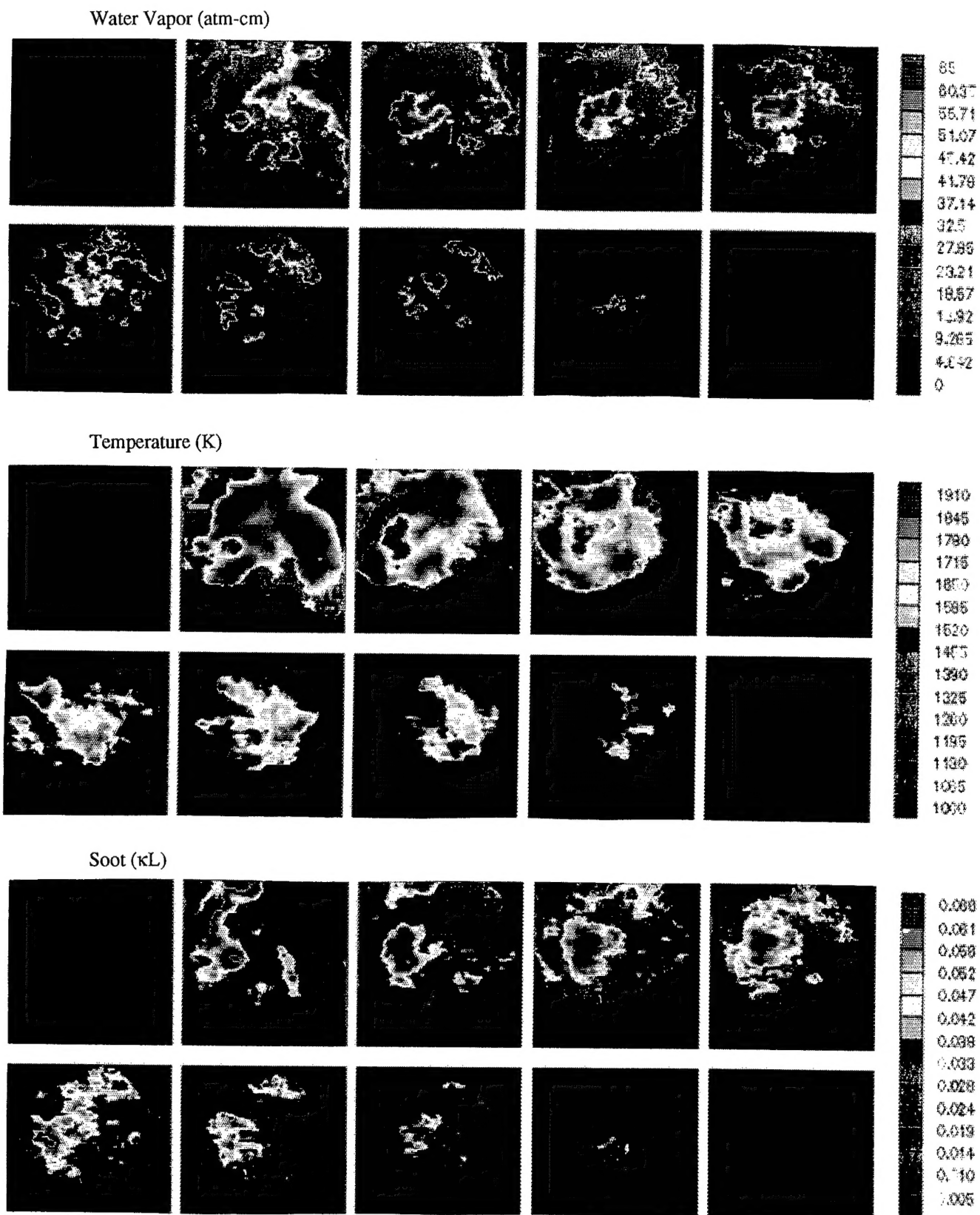


Figure. 12. (B) Distributions of Water Vapor (atm-cm), Temperature (K) and Soot (κL).

regions were interpreted to occur due to the continuous air entrainment expected along the spray axis [21]. Regarding the distributions of water vapor and κL , notably the concentrations are found to be high in the low-temperature zones.

The low κL in those zones may indicate more rapid consumption of soot there, which, however, does not seem to be consistent with the following observation. Since the high temperature zones most probably represent combustion products formed from mixtures with near stoichiometric fuel-air ratios, the water vapor concentration in the corresponding zones should have been also high, which is not the case in the present measurements. The most plausible interpretation of the distributions appears to be a physical factor, which is the high temperature effect on the specific volume of products. Inspecting the data again, when the temperature varies by a factor of two, the concentration inversely changes by about the same value. This finding is most obvious in the later stage of combustion to suggest insignificant impacts by the chemical reactions on the species distributions then.

SUMMARY

Instantaneous distributions of temperature, water vapor and soot were determined in flames by using the Rutgers Super Imaging System (SIS) and new spectrometric methods. Such information may be viewed as "quantitative images."

The SIS permits simultaneous measurement of IR digital images (matrixes) in the same geometrical configuration but in separate spectral bands at successive crank angles at high rates. The spectrometric methods are for processing this raw data to obtain the distributions. These techniques were applied to the investigation of bench-top flames and in-cylinder reactions of both SI and CI engines.

Three new spectrometric methods were presented in this paper: Dual-band mapping method (DBMM); New band-ratio method (NBRM) and Three-band iteration method (TBIM). These methods all employ a new data-based computer program (DBCP) constructed by employing experimental IR data for gaseous species and single-line-group (SLG) model from NASA Handbook (SP-3080).

The concept of DBMM is to find distributions of water vapor and temperature from a mixture when two spectral IR intensity matrices of the mixture are given, which is a reverse process of a common problem of finding the latter when the former are given. Solutions by the method are unique, but errors can be high.

The NBRM is consistent with a few earlier experimental methods employed for temperature measurement in gaseous mixtures. Its concept was conceived during the process of analyzing IR data in the NASA Handbook using the DBCP that the ratio of two spectral intensity of a radiating species in a gaseous mixture is uniquely related to the mixture temperature. Other important characteristics of the method (e.g. pressure effect) were also discovered.

The governing equations of TBIM are basically the Beer's law expressions for three separate species. The three simultaneous equations included absorption coefficients of gaseous species (from DBCP) and those for soot calculated

by the Rayleigh-limit expression plus dispersion equation. Because of the implicit nature of the problem, determination of the final results for each pixel was performed by an iteration method.

Instantaneous spectral intensities of a hydrogen-air flame were processed by both DBMM and NBRM. The results are mutually comparable with each other except for some expected errors by the DBMM. They are also consistent with time-averaged measurements obtained from the similar flame using the sodium-line reversal method as found in literature.

The simultaneous determination of distributions of temperature, water vapor and soot formation was achieved by the TBIM. This was made by processing high-speed spectral IR digital images of a reacting spray plume in a direct-injection CI engine equipped with a high-pressure injection system as operated by Diesel oil (D-2). The results appear to be reasonable in view that any indirect evidence does not challenge the validity and that they are comparable with results by others. The new quantitative images as well as the raw data offer some new insight into the reactions in the cylinder.

ACKNOWLEDGEMENT

The present work has been performed under the sponsorship of the U.S. Army Research Office (Contract No. DAAH04-95-1-0430) and AASERT (DAAH04-94-G-0201), Ethyl Corporation and Ford Motor Company.

REFERENCES

1. Uyehara, O.A. and Myers, P.S., "Flame Temperature Measurements-Electronic Solution of the Temperature Equations," SAE Quarterly Transactions, vol. 1, No. 4, 1947.
2. Matsui, Y., Kamimoto, T., Matusuoka, S., "A Study on the Application of the To-color Method to the Measurement of Flame Temperature and Soot Concentration in Diesel Engines," SAE Paper-800970, 1980.
3. El Wakil, M.M., Myers, P.S., and Uyehara, O.A., "An Instantaneous and Continuous Sodium-line Reversal Pyrometer," ASME Transactions, Paper No. 50-A-94, 1950.
4. Myers, P.S. and Uyehara, O.A., "Accuracy of and Representative Results Obtained with an Infrared Pyrometer Measuring Compression Temperatures," Inst. of Mechanical Engineers, pp. 64-75, 1965.
5. Agnew, W.G., "Two-wavelength Infrared Radiation Method Measures end gas Temperatures near their Peaks," SAE Journal, October 1960.
6. Ferriso, C.C., Ludwig, C.B., and Boynton, F.P., "A Band-ratio Technique for Determining Temperatures and Concentrations of Hot Combustion Gases from Infrared-emission Spectra," 10th Symp. (Int'l) on Combustion, 161, The Combustion Institute, 1965.

7. Ludwig, C.B., Malkmus, W., Reardon, J.E., Thomson, J.A.L., Handbook of Infrared Radiation from Combustion Gases," NASA SP-3080, 1973.
8. Jiang, H., McComiskey, T., Qian, Y., Jeong, Y.I., Rhee, K.T., and J.C. Kent, "A New High-Speed Spectral Infrared Imaging Device Applied for Imaging Gaseous Mixtures from Combustion Devices," Combustion Science and Technology, 90, 5-6, p. 341, 1993.
9. McComiskey, T., Jiang, H., Qian, Y., Rhee, K.T., and Kent, J.C., "High-Speed Spectral Infrared Imaging of Spark Ignition Engine Combustion," SAE Paper-930865, 1993.
10. Jiang, H., Qian, Y. and Rhee, K.T., "High-Speed Dual-Spectra Infrared Imaging," Optical Engineering, 32 (6), pp. 1281-1289, 1993.
11. Clasen, E., Campbell, S., and Rhee, K.T., "Spectral IR Images of Direct Injection Diesel Engine Combustion with High Pressure Fuel Injection," SAE Paper-950605, 1995.
12. Song, K., Clasen, E., Chang, C., Campbell, S., Rhee, K.T., "Post-flame Oxidation and Unburned Hydrocarbon in a Spark-ignition Engine," SAE Paper-952543, 1995.
13. Campbell, S., Clasen, E., Chang, C., and Rhee, K.T., "Flames and Liquid Fuel in an SI Engine during Cold Start," SAE Paper-961153, 1996.
14. Clasen, E., Song, K., Campbell, S., and Rhee, K.T., "Fuel Effects on Diesel Combustion Processes," SAE Paper-962066, 1996.
15. Lewis, B. and von Elbe, G., *Combustion, Flames and Explosions of Gases*, p. 281, Academic Press Inc, 1961.
16. Chang, S.L. and Rhee, K.T., "Computation of Radiation Heat Transfer in Diesel Combustion," SAE Paper-831332, 1983.
17. Bard, S. and Pagni, P.J., Carbon Particles in Small Pool Fire Flame," J. of Heat Transfer, vol 103, pp 357-362, 1981.
18. Dalzel, W.H. and Sarofim, A.F., "Optical Constants of Soot and their Application to Heat Flux Calculation," ASME Trans. vol. 9, p. 100, 1969.
19. Hottel, H.G., Broughton, F.P., "Determination of True Temperature and Total Radiation from Luminous Flames," Industry and Energy Chemistry, 4-2, p. 166, 1932.
20. Abata, D., Stroia, B.J., Beck, N.J., and Roach, A.R., "Diesel Engine Flame Photographs with High Pressure Injection," SAE Paper-880298, 1988.
21. Jeong, Y.I., Qian, Y., Campbell, S. and Rhee, K.T., "Investigation of a Direct Injection Diesel Engine by High-Speed Spectral IR Imaging and KIVA-II," SAE Paper-941732, 1994.